

RESEARCH ARTICLE

The *miR156* juvenility factor and *PLETHORA 2* form a regulatory network and influence timing of meristem growth and lateral root emergence

Marta J. Laskowski^{1,¶}, Helene C. Tiley^{1,*}, Yiling Fang^{1,‡}, Anabel Epstein^{1,§}, Yuyang Fu¹, Roberto Ramos¹, Thomas J. Drummond¹, Renze Heidstra², Priyanka Bhakhri³, Tobias I. Baskin³ and Ottoline Leyser⁴

ABSTRACT

Plants develop throughout their lives: seeds become seedlings that mature and form fruits and seeds. Although the underlying mechanisms that drive these developmental phase transitions have been well elucidated for shoots, the extent to which they affect the root is less clear. However, root anatomy does change as some plants mature; meristems enlarge and radial thickening occurs. Here, in *Arabidopsis thaliana*, we show that overexpressing *miR156A*, a gene that promotes the juvenile phase, increased the density of the root system, even in grafted plants in which only the rootstock had the overexpression genotype. In the root, overexpression of *miR156A* resulted in lower levels of *PLETHORA 2*, a protein that affects formation of the meristem and elongation zone. Crossing in an extra copy of *PLETHORA 2* partially rescued the effects of *miR156A* overexpression on traits affecting root architecture, including meristem length and the rate of lateral root emergence. Consistent with this, *PLETHORA 2* also inhibited the root-tip expression of another *miR156* gene, *miR156C*. We conclude that the system driving phase change in the shoot affects developmental progression in the root, and that *PLETHORA 2* participates in this network.

KEY WORDS: *Arabidopsis thaliana*, Carbon sequestration, Lateral root, Meristem development, Phase change, *PLETHORA*

INTRODUCTION

In *Arabidopsis thaliana*, progression from the juvenile to the adult state is regulated by a network of microRNA genes, including those that code for *miR156*, which is expressed at high levels in juvenile plants, and *miR172*, which increases in level as plants mature (Wu et al.,

2009). The change in *miR156* expression that occurs with age involves an increase in repressive H3K27me3 histone marks associated with *miR156A* and *miR156C* (Xu et al., 2016b, 2018a,b). Mutants that are impaired in their ability to place these marks show delayed phase transitions (Xu et al., 2016b).

Expression of *miR156* affects plant development by targeting mRNAs for destruction. Specifically, *miR156* transcripts target genes in the *SQUAMOSA PROMOTER BINDING PROTEIN-LIKE* (*SPL*) family, decreasing *SPL* expression (Yu et al., 2012; Xu et al., 2016a). Among the genes induced by *SPLs* are the *miR172* family of microRNA genes. Thus, reduced expression of *miR156* leads to an increase in *miR172* gene expression, which promotes adult characteristics in the shoot (Wu et al., 2009). Although most well understood in *A. thaliana*, this network of small RNAs appears to control phase transitions in many species (Wang et al., 2011; Poethig, 2013).

Root development is also affected by the *miR156* family of genes. The *miR156* family comprises genes that code for nearly identical mature miRNAs, with individual genes being differently expressed; several *miR156* genes are expressed in the root apical meristem and in lateral root meristems (Yu et al., 2015; Barrera-Rojas et al., 2020; Cheng et al., 2021). However, overexpression of *miR156* reduces the number of cortical cells in the meristem (Barrera-Rojas et al., 2020). Supporting the observation that *miR156* can reduce meristem size are data showing that levels of *miR156* are low in areas of active cell division (Cheng et al., 2021). Additionally, overexpression of *miR156* affects root development by accelerating the emergence of initiated root primordia (Yu et al., 2015). Downstream of *miR156*, changes in expression of *SPL10*, a target of *miR156*, have also been shown to affect growth of the primary root (Gao et al., 2018; Barrera-Rojas et al., 2020). These effects of *miR156* expression share the common thread of affecting the meristem and growth zone of primary or lateral roots.

Another gene family that profoundly affects meristem development is the *PLETHORA* (*PLT*) family of transcription factors. Root meristems form at many points during development; the primary root meristem forms in the embryo and other meristems arise after germination. When meristems develop from callus or during lateral root formation, three *PLETHORA* family transcription factors, *PLT3*, *PLT5* and *PLT7* are expressed early in the process. These *PLTs* are required for the subsequent expression of *PLT1* and *PLT2* (Kareem et al., 2015; Hofhuis et al., 2013; Du and Scheres, 2017). Expression of *PLT1* and *PLT2* activates genes required for the progression of meristem formation, and also allows the stem cells and meristem to persist (Du and Scheres, 2018; Aida et al., 2004; Galinha et al., 2007). In established primary root meristems, *PLT* proteins contribute to a protein complex that induces *WOX5*, which, in turn, maintains neighboring cells as stem cells (Shimotohno et al., 2018; Sarkar et al., 2007; Pi et al., 2015).

¹Biology Department, Oberlin College, Oberlin, OH 44074 USA. ²Cluster of Plant Developmental Biology, Laboratory of Molecular Biology, Wageningen University & Research, Droevendaalsesteeg 1, 6708 PB Wageningen, The Netherlands.

³Department of Biology, University of Massachusetts, Amherst, MA 01003, USA.

⁴Sainsbury Laboratory, University of Cambridge, Cambridge, CB2 1LR, UK.

*Present address: USDA, Agricultural Research Service, Mycotoxin Prevention and Applied Microbiology Research Unit, National Center for Agricultural Utilization Research, Peoria, IL 61604, USA. [‡]Present address: Department of Plant and Microbial Biology, University of California, Berkeley, CA 94720, USA. [§]Present address: University of Miami Miller School of Medicine, Miami, FL 33136, USA.

¶Author for correspondence (mlaskows@oberlin.edu)

 M.J.L., 0000-0002-8875-7627; H.C.T., 0000-0002-4227-1824; Y.F., 0000-0001-6051-9320; R.H., 0000-0001-9032-5770; P.B., 0000-0003-0916-8814; O.L., 0000-0003-2161-3829

This is an Open Access article distributed under the terms of the Creative Commons Attribution License (<https://creativecommons.org/licenses/by/4.0>), which permits unrestricted use, distribution and reproduction in any medium provided that the original work is properly attributed.

Handling Editor: Ykä Helariutta

Received 8 June 2021; Accepted 20 September 2022

As roots age, both the meristem and elongation zone enlarge (Beemster and Baskin, 1998), an increase that could be related to changes in *PLT* gene expression. High levels of *PLT* expression in the root tip are present in the stem cells and these levels progressively decrease toward the shootward end of the elongation zone (Galinha et al., 2007). High levels of *PLT2* increase the length of the meristem and repress elongation of individual cells (Mähönen et al., 2014). Shootward of the stem cell niche, the level of *PLT2* reaches a threshold at the point where cell division slows and expression of some markers of differentiation begins (Salvi et al., 2020). A negative regulatory loop between *PLT2* and the cytokinin response factor *ARR12* participates in setting the location of this boundary between the meristem and the transition zone (Salvi et al., 2020). Growth of the meristem is also restricted by the cytokinin response factor *ARR1* (Moubayidin et al., 2010, 2016).

Here, we consider the possibility that the enlargement of the growth zone that occurs during the first few days after germination may be driven by increases in *PLT2* expression. We examine the extent to which this and other changes in root developmental traits are coordinated by *miR156* and discover that *miR156* regulation of *PLT2* is partially responsible for some of the phenotypes associated with high levels of *miR156*. The data also uncover a regulatory network through which *miR156C* and *PLT2* repress one another.

RESULTS

Overexpression of *miR156A* increases the density of roots in the mature root system

Overexpression of *miR156* has highly pleiotropic effects on shoot growth, including more rapid production of rosette leaves (Wu and Poethig, 2006; Wu et al., 2009). To determine the extent to which overexpression of *miR156A* specifically affects root development, *35S::miR156A* plants were reciprocally grafted to wild type and grown to maturity in soil-filled rhizotrons. Plants in which both roots and shoots were genotypically *35S::miR156A* were substantially larger than wild type; the shoots had more leaves and the roots were more densely packed (Fig. 1A,B). Grafting wild-type rootstock onto a *35S::miR156A* shoot resulted in an intermediate root system phenotype; the root system was less dense than when *35S::miR156A* was self-grafted, but somewhat more dense than when wild type was self-grafted (Fig. 1C). This indicates that the shoot system plays some role in establishing the density of the root system. To determine whether the increased root system resulted entirely from a larger shoot, *35S::miR156A* rootstock was grafted onto wild-type shoots. Once again, the root systems took on an intermediate phenotype (Fig. 1C). *35S::miR156A* roots with wild-type shoots were less dense than those of *35S::miR156A* self-grafts but denser than those produced by wild-type self-grafts, indicating that the level of *miR156A* expression in the root affects root development.

Expression of *miR156A* and *miR156C* declines after germination

To examine the pattern of *miR156* expression in the days immediately following germination, we used previously described lines expressing *pmiR156A::GUS* and *pmiR156C::GUS* reporter constructs (Barrera-Rojas et al., 2020). For the time-course experiments described here and throughout this paper, seeds were examined at 12 h intervals after plating to determine the time of germination; all ages are reported as time since germination.

The level of *miR156A* and *miR156C* expressed in the root tip declined from day 1, when roots were almost entirely stained, to day

9 (Fig. 2A,B). In the root cap, expression of both *miR156A* and *miR156C* decreased until staining was no longer visible. Staining in the growth zone (meristem plus elongation zone) also decreased, but remained visible. For *miR156A*, expression shootward of the growth zone became patchy before disappearing (Fig. 2C,D), whereas for *miR156C*, staining shootward of the growth zone persisted, particularly in the central vasculature (Fig. 2E-H). Expression of *miR156A* and *miR156C* during lateral root formation was variable. However, *miR156A* staining was generally not visible in outer layers of the primordia from the time primordia contained three layers of cells through emergence (Fig. 2D). For *miR156C*, staining was visible in stage 1 and stage 2 lateral root primordia (Fig. 2E,F) and not visible in recently emerged lateral roots (Fig. 2G); intermediate stages showed variable levels. Longer emerged lateral roots showed expression of *miR156C* behind the tip (Fig. 2H).

Expression of *PLT2*, but not *PLT3*, varies with age of the plant and level of *miR156A* expression

We followed the expression of *PLT3*, a gene that is expressed early in lateral root development, by using a 4.5 kb *PLT3::GUS* transcriptional reporter. On day 1, β -glucuronidase (GUS) staining in the primary root was strong throughout the meristem and root cap (Fig. 3A, top row). Expression of *PLT3::GUS* shootward of the quiescent center declined rapidly as the roots matured. To determine whether this decline in *PLT3* expression is driven by increasing maturity of the root, the *PLT3::GUS* reporter was crossed to *35S::miR156A* (Wu and Poethig, 2006). Overexpression of *miR156A* did not change the expression of *PLT3::GUS* detected in the root tip during this period (Fig. 3A,B). Consistent with these results, real-time PCR levels of *PLT3* in the *miR156A*-overexpressing line on day 2 were observed to be 1.3 ± 0.2 (mean \pm s.d.) times those of wild type.

Expression of a typically late-expressed *PLT* gene (*PLT2*) was observed in root tips of a wild-type line carrying a *PLT2*-Venus fluorescent fusion protein driven by the native promoter (Fig. 3C, top row). On day 1, *PLT2*-Venus was expressed mainly in the root cap and the stem cell niche. On day 2, expression expanded shootward. The intensity of expression also increased, reaching a peak around day 4 (Fig. 3C,D). The level of *PLT2*-Venus then fell from around day 4 to day 7.

We crossed the *PLT2*-Venus reporter into the *35S::miR156A* line. In this line, the level of *PLT2*-Venus in *35S::miR156A* was modestly lower than that of wild type at day 1, and the rapid increase that occurred in wild type was delayed, resulting in substantially lower levels around days 3 and 4 compared with wild type (Fig. 3C,D). Similar to wild type, levels of *PLT2*-Venus in *35S::miR156A* fell between about 4 and 7 days (Fig. 3D). At day 4, the level of *PLT2*-Venus fluorescence in *35S::miR156A* plants was still rising whereas the level in wild type was not. Thus, *35S::miR156A* reduced the initial level of *PLT2*-Venus expression and delayed and reduced its subsequent increase.

PLT2 represses *miR156C*

The spatiotemporal pattern in which signal from *pmiR156C::GUS* declined (Fig. 2A) raised the question of whether *PLT2* might modulate expression of this small RNA. In the wild-type background on day 4, high levels of *pmiR156C::GUS* staining were observed just shootward of the quiescent center (Fig. 4B,C). Expression of *miR156C* then declined somewhat through the meristem, increasing again near the start of the elongation zone. Rootward of the quiescent center, expression of *miR156C* also declined before increasing again in the outer layers of columella cells (Fig. 4C). The regions near the quiescent center that had lower

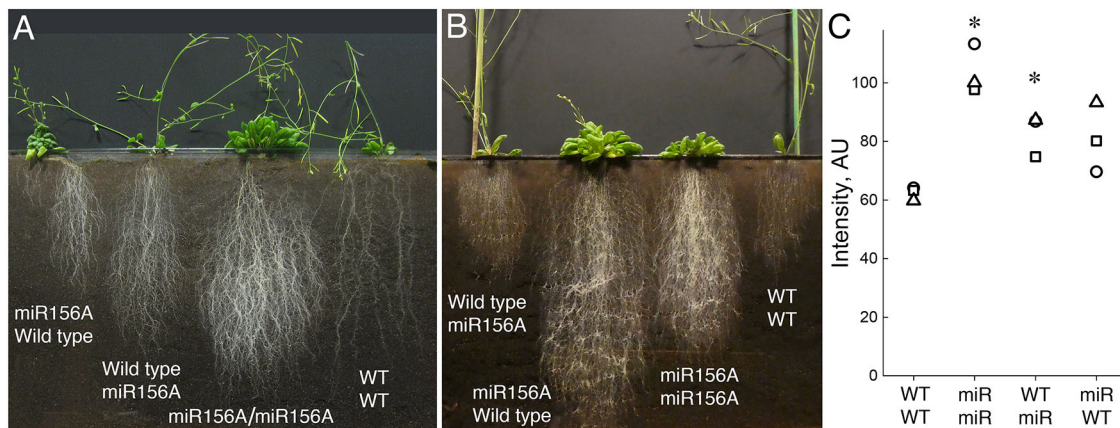


Fig. 1. Expression of *miR156A* affects root development in a partially root-autonomous manner. Labels give shoot genotype over root genotype with *miR156A* standing for *35S::miR156A*. (A,B) Images of two of the rhizotrons at maturity. (C) Quantification of root density based on image analysis. Each symbol represents the average intensity of the entire root system for one plant in a given rhizotron. Data for three complete rhizotrons are given here. Asterisks indicate that the mean differs significantly from wild type (equivalence with wild type was rejected with $P < 0.05$ in a two-tailed Student's *t*-test).

levels of staining were also regions in which *PLT2* was expressed (Fig. 3C).

To check whether *miR156C* is affected by *PLT2* expression, we crossed *pmiR156C::GUS* to the *plt2-3* CRISPR allele and observed GUS staining in F3 seedlings on day 4 (Fig. 4A,C). Throughout the measured region, GUS stained *plt2-3* plants somewhat more strongly than wild-type lines, although the difference was larger in the meristem and in the region just shootward of the meristem. The increased staining in *pmiR156C::GUS* roots in the *plt2-3* background indicates that *PLT2* represses expression of *miR156C* in

the root tip, at least on day 4 when *PLT2* levels in wild-type roots are high.

The effect of *miR156* overexpression on root system architecture acts in part through *PLT2*

Because *35S::miR156A* plants had reduced *PLT2*-Venus expression (Fig. 3), we hypothesized that increasing the dosage of *PLT2* by crossing in *PLT2*-Venus might limit the effect of *35S::miR156A* on root architecture. To assess root architecture, we grew plants to maturity in rhizotrons (in this case without grafting). As before, *35S::*

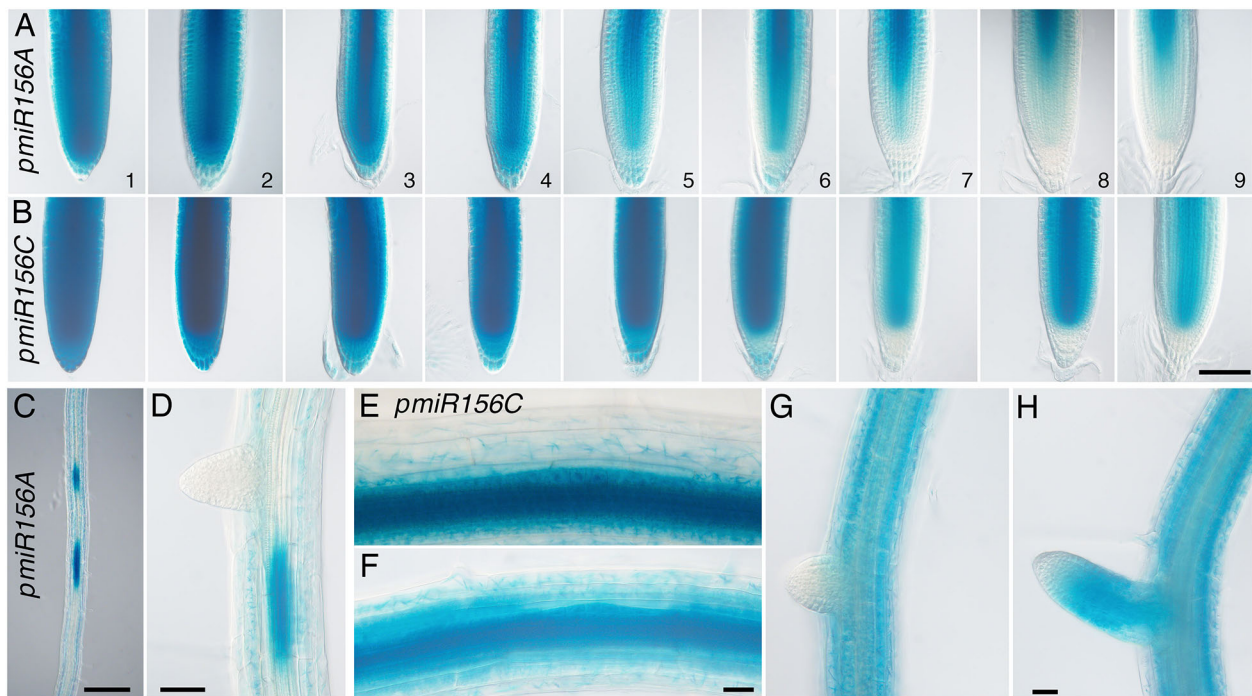


Fig. 2. Expression of *miR156A* and *miR156C* in the root tip decline as roots mature. (A,B) Representative primary roots from day 1-9 expressing (A) *pmiR156A::GUS* or (B) *pmiR156C::GUS*. Nine to 11 roots per genotype were examined each day. (C,D) Shootward of the tip, staining in *pmiR156A::GUS* became patchy (C) and was not present in a recently emerged lateral root (D). (E-H) Lateral root primordia in *pmiR156C::GUS*-expressing lines were stained at stage 1 (E) and stage 2 (F) but not when recently emerged (G). (H) Staining appeared behind the tip in longer emerged lateral roots. Roots were examined in two separate trials with similar results. Roots were stained overnight except for *pmiR156A::GUS* in C, which was stained for 3 h. Scale bars: 100 μ m (A,B); 200 μ m (C); 50 μ m (D); 25 μ m (E,F); 50 μ m (G,H).

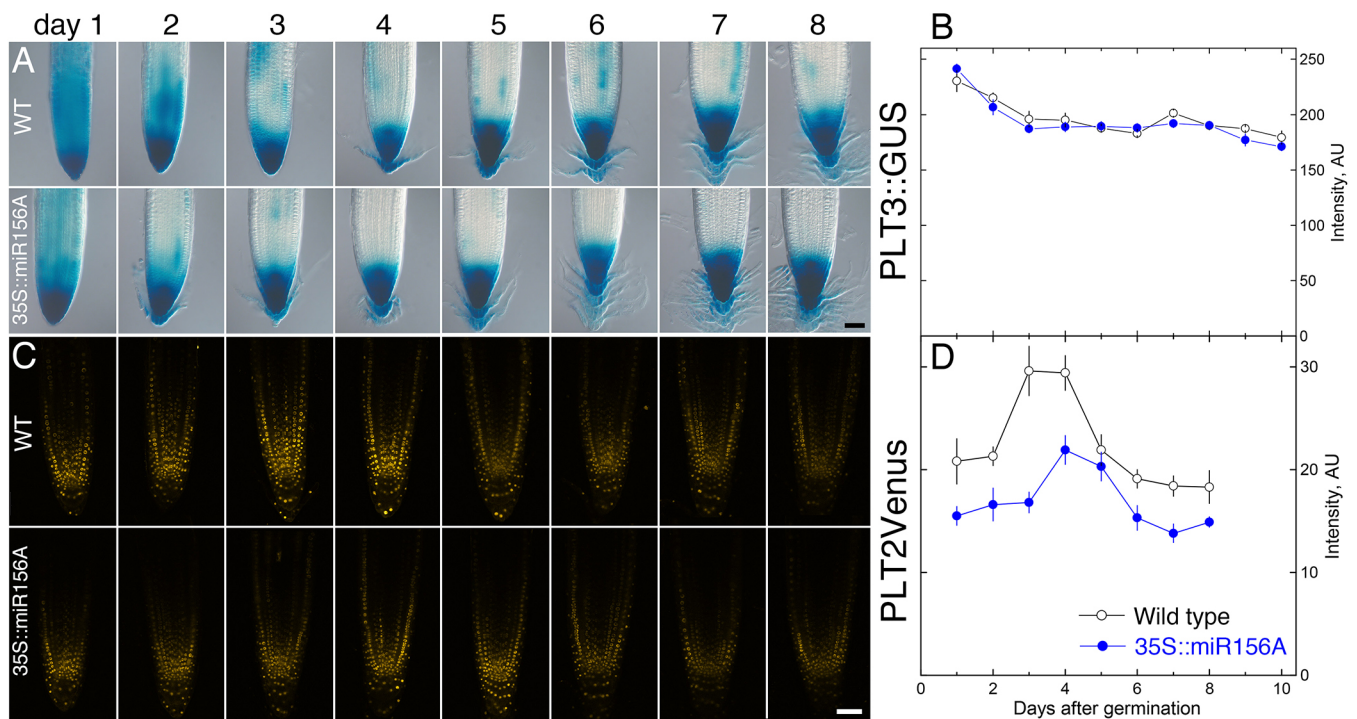


Fig. 3. *PLT* expression changes as plants mature and in response to the level of *miR156A*. (A) Brightfield micrographs of root tips expressing *pPLT3::GUS* at days 1-8 in wild type (WT; top) and *35S::miR156A* (bottom). Scale bar: 50 μ m. (B) Mean intensity of *PLT3::GUS* in a region of fixed size that covered the root cap and stem cell niche. Symbols represent mean of eight to ten roots \pm s.e.m. (C) Confocal fluorescence micrographs of *pPLT2::PLT2-Venus* in wild-type root tips (WT; top) and in *35S::miR156A* (bottom) on days 1-8. Scale bar: 50 μ m. Eight new roots from the same cohort were imaged each day using ZEN black software (Zeiss) in a tile-scan mode with consistent settings. (D) Time course of fluorescence intensity in a region of fixed size that covered the stem cell niche. Symbols represent mean \pm s.e.m.

miR156A plants had substantially denser root systems than did wild-type plants (Fig. 5). Wild-type plants expressing *PLT2-Venus* had root systems that appeared to be a bit shorter than those of wild-type plants without the added copy of *PLT2*, but these shallower root systems did not appear to be substantively different from wild type in terms of their root density (Fig. 5B). In contrast, *35S::miR156A* plants carrying *PLT2-Venus* had root systems that were noticeably less dense than those lacking the added copy of *PLT2*. Thus, the line carrying *PLT2-Venus* partially reversed the *miR156* overexpression phenotype. Crossing in *PLT2-Venus* also affected the shoot system, with flowering occurring earlier than for *35S::miR156A* alone. Conversely, introducing the *plt2-3* mutant into *35S::miR156A* slightly increased the average root density in this experiment (Fig. 5B), which is consistent with lower levels of *PLT2* expression conferring some of the *35S::miR156A* overexpression phenotype. Together, these data suggest that a substantial portion of the increased density of *35S::miR156A* root systems is attributed to *PLT2*.

Expression of *miR156* and *PLT2* contribute to the length of the meristem and elongation zone

To examine the effect of *miR156* on development of the root system in more detail, we analyzed growth kinematically, obtaining parameters of interest from the velocity profile (Baskin and Zelinsky, 2019; see Materials and Methods). The length of the meristem was of particular interest because overexpression of *miR156* is associated with lower levels of *PLT2*, and in several *plt* mutants, including *plt1plt2* double mutants, the meristem becomes shorter and can be lost as the plants mature (Galinha et al., 2007).

In wild-type plants, the length of the meristem, the length of the growth zone and overall root growth increased substantially from

day 2 to day 6 (Fig. 6). In *miR156A*-overexpressing plants, the lengths of the meristem and growth zone were initially longer than wild type (Fig. 6C,D). The rate of cell proliferation, measured in a separate experiment, was generally higher than in wild type, although day 1 did not show a significant effect (Fig. S1). However, in *35S::miR156A*, the longer meristem was not maintained and by day 6 both the meristem and the growth zone were notably shorter than those of the wild type. Adding a copy of *PLT2-Venus* to *35S::miR156A* plants largely reversed this effect, restoring the initial length of these zones to that of wild type and permitting the zones to increase in length from day 2 to day 4 (Fig. 6). These data support the idea that the effect of *miR156* on the length of the meristem acts at least partially through its effect on *PLT2* expression.

To test further whether elongation of the growth zone might be regulated by the phase of the plant, we investigated the *tem1tem2* double mutant, which has elevated levels of the *miR172* maturity factor (Aguilar-Jaramillo et al., 2019). The growth rate of these plants increased faster than wild type (Fig. 6A). Relative expansion rate remained similar to that of wild type, but the length of the meristem, as well as the total length of the growth zone, increased more rapidly than in the wild type (Fig. 6B,D). These data support the idea that longer growth zones are a feature of more mature plants.

In a separate set of experiments, the rate of cell production was calculated from the ratio of root growth rate to the length of mature cortical cells (Baskin, 2013). The higher-than-wild-type growth rate of the *tem1tem2* double mutant was associated with a higher-than-wild-type rate of cell production (Fig. S1). Because cell production rate also increased as wild-type plants aged, these data also support the idea that the meristems of *tem1tem2* plants accelerate developmental transitions seen in the wild-type root growth zone.

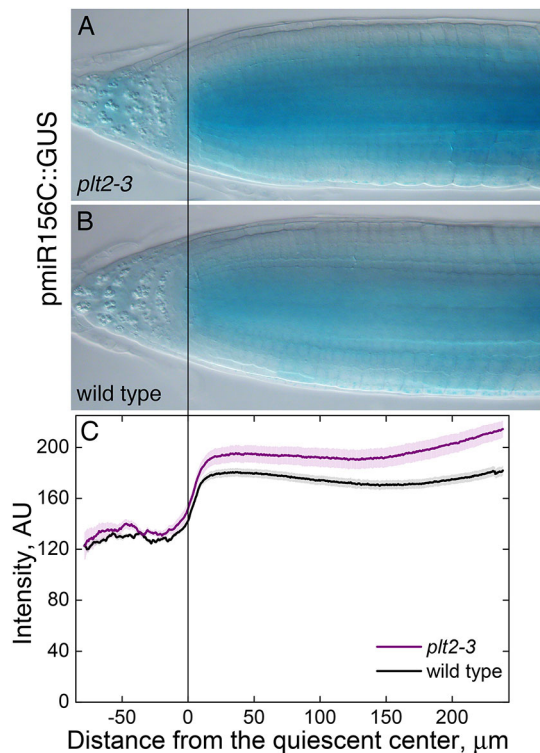


Fig. 4. *PLT2* represses expression of *miR156C*. (A,B) Representative images of day 4 *plt2-3* (A) and wild-type (B) roots carrying *pmiR156C::GUS*, after staining for 45 min and clearing in chloral hydrate. (C) Intensity profiles were determined by averaging profile plots, for a line width of 40 pixels, obtained from ImageJ on an inverted red channel image. Profiles were made by combining data for one line extending from the quiescent center rootward through the root cap and a second line from the quiescent center extending shootward for 27 *plt2-3* and 37 wild-type roots. Shaded area represents s.e.m. The experiment was repeated with a 3 h staining time and gave a generally similar result.

Lateral root production and development

Having examined the effect of phase regulators on development of the root apical meristem, we were interested in knowing the extent to which the formation of lateral root meristems might be affected by the maturity of the plant. To separate effects of plant maturity from the developmental progression undergone by individual lateral root primordia, we marked the position of the root tip each day for 10 days, numbering the segments between marks from 1 (oldest) to 10 (youngest). We followed expression of *PLT3* in the forming lateral root meristems using the *PLT3::GUS* reporter line. Because *GUS* staining is lethal, we removed a sample of roots each day and counted the numbers of lateral root primordia and emerged laterals in each segment. Data from one such experiment are shown in Fig. 7A.

As expected, we observed that the number of *PLT3::GUS* expressing spots – presumptive lateral root primordia – increased during the first 2 days after a segment formed (Fig. 7A, dark-blue bars). The number of *PLT3::GUS*-expressing spots then declined on the third or fourth day after a segment formed. Although some of this decline was accounted for by primordia developing into emerged lateral roots (light-colored bars), emergence does not account for all of the loss. In fact, based on examination through a compound microscope, segments that were at least 3 days old had numerous unstained lateral root primordia, indicating that *PLT3* expression is repressed in some primordia after a few days.

To determine whether the maturity of the plant affects the progression of lateral root development, we investigated whether the time at which lateral root primordia lose their *PLT3::GUS* expression varied with the age of the plant. Based on three trials, of which the data in Fig. 7A are one, the average number of stained areas in segment 1 tended to decline steadily over time, reaching a minimum 7.3 days after the segment formed. In subsequent segments, the loss of staining reached its greatest extent approximately 4 days after the segment formed. Specifically, the number of *PLT3::GUS*-stained spots reached a minimum 4 ± 1.0 days after segment 2 formed, and 3 ± 1 days, 4.3 ± 1.5 days and 4 ± 0 days after segments 3, 4 and 5 formed, respectively. These data indicate that, with the notable exception of segment 1, the decrease in the number of *PLT3::GUS*-stained spots appears to be a sequential part of the process of forming a new lateral root, little affected by the age of the plant.

Area of *PLT3::GUS* expression in lateral root primordia varies as plants mature

In addition to the number of *PLT3::GUS*-expressing spots, the size of each spot also changed as the plants matured and this feature was found to vary with the age of the plant. Unlike the previous metric, which was followed in individual segments over time, the area occupied by *PLT3::GUS* stain was measured on the segment of root that formed in the most recent 24 h, i.e. the root tip. For a plant that was 2 days post-germination, we looked at segment 2, and for a plant that was 3 days post-germination, we looked at segment 3, and so on. In this way, the youngest tissue in plants of one age was compared with the youngest tissue in plants at the next age. In this youngest tissue, the area of individual *PLT3::GUS*-stained spots increased as the age of the plant increased (Fig. S2A). The stained area increased steadily for roughly the first 4 days, and then appeared to plateau.

In the segment of root that formed 1 day before the youngest segment (e.g. segment 3 on a plant that is 4 days-post germination), the area of each stained spot increased slightly between days 1 and 2, and then declined (Fig. S2B). The decline in the size of *PLT3::GUS*-stained spots in lateral root primordia mirrored the decline in *PLT3::GUS* seen in the primary root tip (Fig. 3B). Evidently, the area of *PLT3::GUS* staining in lateral root primordia is affected by the age of the plant, with a notable inflection around day 4, although the specific patterns depended on the age of the segment.

Lateral root emergence is accelerated by *35S::miR156A* and inhibited by *PLT2*

The kinetics of lateral root emergence in wild-type roots can be visualized by replotting the data in Fig. 7A to show the percentage of emerged laterals for segments of interest (Fig. 7B). The length of time required for lateral root primordia to emerge decreased as roots matured. This can be seen in Fig. 7B by comparing the slopes of the lines representing segment 1 (light blue) and segment 4 (black). On segment 1, the rate of lateral root emergence was relatively slow and laterals continued to emerge even by day 10, at which time about 30% of the primordia on the segment had emerged. As the root aged, the rate of emergence rose, so that by segment 4, roughly half of the primordia on the segment emerged in a single day.

Despite the fact that lateral roots emerged more rapidly as roots matured (Fig. 7B), plants that overexpress *miR156* emerge lateral roots more rapidly than wild type (Yu et al., 2015). We confirmed this finding by counting the number of emerged lateral roots on segments 1, 2 and 3 over time in wild type and *35S::miR156A* (Fig. 8). This established a paradox as both more mature root segments and roots that overexpress a juvenility factor emerge lateral roots more rapidly.

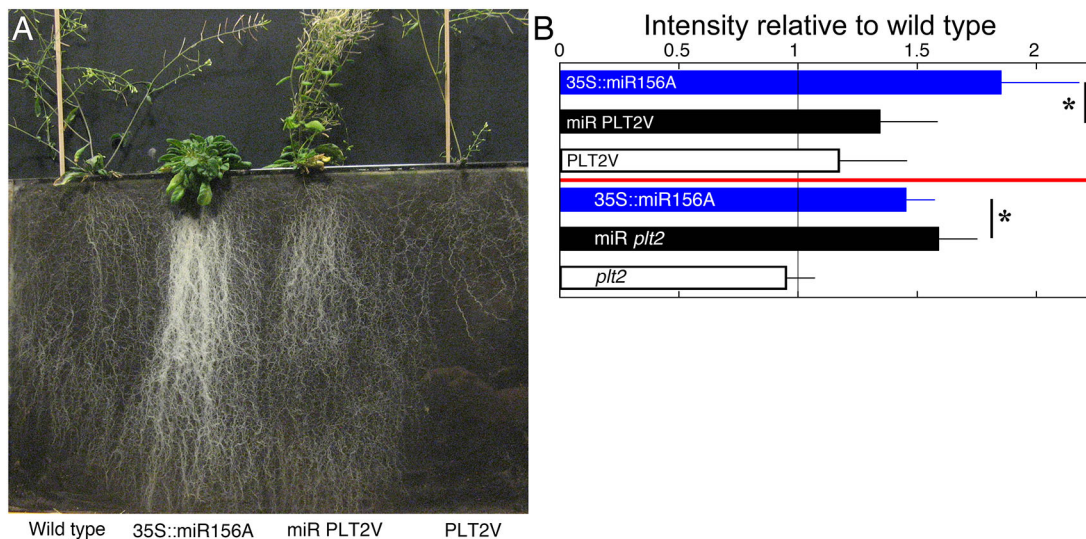


Fig. 5. PLETHORA expression contributes to phase identity. (A) Rhizotron showing the effect on root system architecture of adding *PLT2-Venus* to wild type and *35S::miR156A*. (B) Root system density. Bars represent mean density of root systems, calculated as described in Fig. 1. Top: Bars represent mean density \pm s.d. for five rhizotrons $*P < 0.05$ (density of *35S::miR156A PLT2-Venus* root system equaling that of *35S::miR156A* rejected by a two-tailed Student's *t*-test). The experiment was repeated with a similar result. Bottom: Bars represent mean \pm s.e.m. for 15 rhizotrons. $*P < 0.05$ (density of *35S::miR156A plt2-3* root system equaling that of *35S::miR156A* rejected by a two-tailed Student's *t*-test).

We wondered if this situation might arise from *PLT2*, insofar as *PLT2* is expressed as a bell-shaped curve with lower levels in both older wild-type plants and in younger plants that overexpress *miR156A* (Fig. 3D). To check, we compared the rate of lateral root emergence in *35S::miR156A* lines with and without *PLT2-Venus* crossed in, and found that the additional *PLT2-Venus* gene effectively restored the rate of lateral root emergence essentially to that of the wild type in all three of the root segments examined (Fig. 8).

In wild-type plants, *PLT2* delayed the appearance of emerged lateral roots

If *PLT2*-mediated repression of lateral root emergence occurred predominately during the brief peak of *PLT2* expression around day 4, it might shift the age at which lateral roots emerge. To see if this were the case, emerged lateral roots were counted in wild type and *plt2-3*. For this analysis, only the portion of primary root that grew by the end of day 3 (segments 1-3) was considered. The average number of emerged roots that formed on this portion of the root in wild type and *plt2-3* appeared similar at day 8; however, on days 4 and 5 the *plt2-3* loss-of-function mutant had more lateral roots than did wild type (Fig. 9A). Thus, the presence of *PLT2* delayed the age at which emerged lateral roots appear.

PLT gene expression delayed the appearance of elongated leaves

Having identified roles for *PLT* expression in the timing of root development, we wondered whether *PLT* genes might also regulate the timing of any developmental events in the shoot. As *A. thaliana* plants mature, the shape of successive leaves gradually progresses from round to oblong (Wu and Poethig, 2006). Our data confirm this progression from round leaves (aspect ratio near 1) to a more elongated form (aspect ratio near 2; Fig. 9B). A progression similar to that of the wild type was seen in a loss-of-function mutant of *PLT4* (*babyboom 1-1*). As previously described, the first two leaves of a *plt3plt5plt7* triple mutant show no difference from wild type (Radhakrishnan et al., 2020). However, in older leaves, the *plt3plt5plt7* triple mutant took on a more mature aspect more

rapidly than did wild type (Fig. 9B). Evidently, absence of these three 'early' *PLT*s accelerates maturation of leaf shape. Thus, in the shoot, these *PLT*s retard this aspect of maturation. These data, and the data showing that *PLT2* affects the age at which emerged lateral roots appear, indicate that *PLT* genes affect the age at which some developmental events occur throughout the plant.

DISCUSSION

We investigated the possibility that roots undergo phase change by characterizing how a pivotal regulator of plant phase, *miR156*, and a known regulator of meristem activity, *PLT2*, influence root development. Overexpression of *miR156* increases the density of the root system (Figs 1, 5). Our data further show that expression of *PLT2* and the *miR156* family are linked by a mutually repressive regulatory network (Figs 3-5). Because *PLT2* is expressed at high levels for a brief period of time, its effects on meristem development (Fig. 6) and lateral root emergence (Figs 8, 9) are restricted to specific developmental stages. Our model of how these factors work together to regulate root development is shown in Fig. 10.

Evidence for *PLT2* involvement in the phase-regulated *miR156* network

The data presented here indicate that *PLT2* and *miR156* form a regulatory loop in which each represses expression of the other. Repression of *PLT2* by *miR156* is shown in Fig. 3 and is consistent with the observation that *PLT2-Venus* partially rescues the effects of *miR156A* overexpression (Figs 5, 6, 8). Mature *miRNA* transcripts target mRNAs for destruction by binding to regions of mRNA with complementary sequences. Although *PLT2* and *miR156C* have a 10-base-pair-long region of alignment, there is as yet no evidence that this pairing has a functional significance. The reported targets of *miR156* are in the *SPL* family, which suggests that the effect of *miR156C* on *PLT2* is indirect.

Evidence that *PLT2* represses *miR156C* is seen in the expression of *miR156C::GUS* (Fig. 4). *PLT2* binds genomic DNA 1.1 kb upstream of another *miR156*, *miR156D* (Santuari et al., 2016). Like *miR156C*, *miR156D* is expressed in root meristems (Yu et al.,

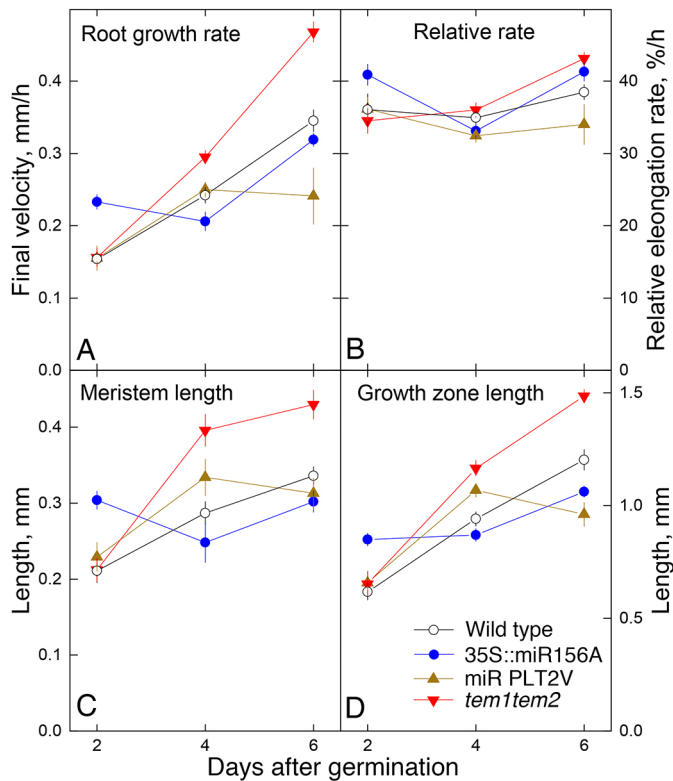


Fig. 6. Development of the growth zone is affected by known phase-change regulators. (A-D) Average growth rate (A), relative elongation rate (B), length of the meristem (C) and length of the growth zone (meristem+elongation zone) (D), for wild-type roots and those of 35S::miR156A, 35S::miR156A with PLT2-Venus, and tem1tem2. Symbols represent mean±s.e.m. for eight to 11 roots. As used here, 'meristem' includes a transitional zone where cells were not elongating rapidly. Plotted parameters were obtained from the velocity profile as described in Materials and Methods.

2015). Although motifs resembling the PLT2-binding consensus do exist near *miR156C*, binding was not reported to be above the designed threshold for the experiment (Santuari et al., 2016). In addition, PLT4 (BBM) has been shown to bind the *miR156C* and *miR156D* genes (Horstman et al., 2015, 2017). Thus, PLTs may affect expression of several *miR156* genes in the root meristem.

PLT2 may also induce expression of some *miR172* genes, a microRNA family associated with shoot maturation. A whole-genome study of PLT2 binding identified a PLT2-binding site 446 bp before the transcription start site of *miR172E*, and about 1.5 kb after the start sites of *miR172A* and *miR172D* (Santuari et al., 2016). In addition, overexpressing *PLT2* reduced the level of the *miR172* targets *SNZ*, *SMZ* and *TOE1* (Santuari et al., 2016). PLT2 binding was not reported near *SNZ* or *SMZ* (Santuari et al., 2016) further strengthening the idea that *PLT2* represses these genes by inducing *miR172*. Our attempts to confirm a difference in levels of pre-*miR172* in wild type and *plt2-3* by qPCR in day 6 root tips were hampered, at least in part, by overall low levels of expression. However, the published data raise the possibility that PLT2 may serve as a switch, repressing the *miR156* juvenility factor and inducing *miR172*.

Potential for adaptive significance

It appears that the level of *PLT2* expression affects the balance between promoting growth at the present moment and generating the potential for future growth, and the optimal trade-off between

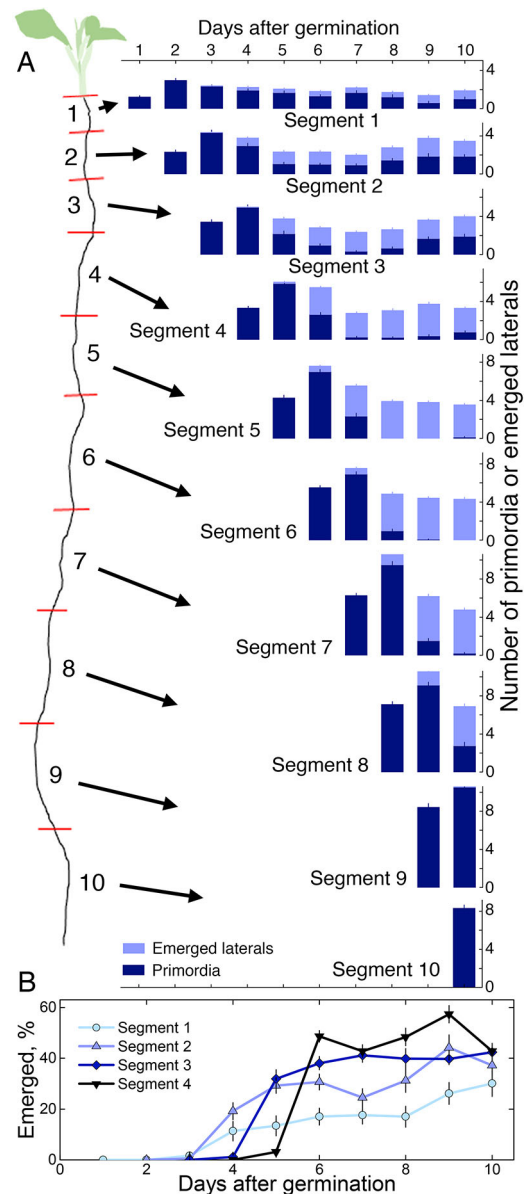


Fig. 7. Rates of lateral root production and development vary as plants mature. (A) Drawing on the left illustrates the sampling approach. Root growth was marked daily; the portion of root that grew in the first day post germination was called segment 1, and so on. The shootward end of segment 1 was defined as the hypocotyl junction, functionally the end of the region bearing dense root hairs. The number of *PLT3::GUS*-staining lateral root primordia and emerged lateral roots per segment was recorded daily following an overnight stain. Bars represent mean±s.e.m. for 26-43 roots per day. (B) Subsets of the data in A replotted to show the rate of lateral root emergence measured as the percentage of lateral root primordia on the indicated segment that have emerged as a function of the age of the plant; for each segment, the number of primordia when that segment was 2 days old was used as the baseline. Data in this figure are from a single experimental trial. Error bars represent s.e.m.

these states may vary as the plant matures. Because levels of *miR156C* are high at germination, expression of *PLT2* is expected to be strongly repressed. Indeed, levels of PLT2 protein were low in the first day or two after germination (Fig. 3D). High levels of PLT2 repress the rate of cell elongation (Mähönen et al., 2014). Therefore, low levels of PLT2 around the time of germination should allow the rate at which existing cells elongate to increase, promoting

elongation of the radicle and allowing the root to emerge from the seed and reach the soil more rapidly, a factor that could be advantageous at this early stage of the life cycle. However, if the total level of *PLT* expression remains low for too long, the meristem may fail to maintain its length (Galinha et al., 2007). The regulatory relationship between *miR156C* and *PLT2* provides for a subsequent increase in *PLT2* expression that allows the meristem to enlarge, setting the stage for a robust level of future growth (Fig. 10).

Relationship of an auxin pulse from the shoot to the development of the growth zone

Considerable evidence supports the idea that a pulse of auxin is transported from the shoot to the root shortly after germination, and it is interesting to consider how that pulse might interact with the developmental changes observed here. Two separate studies detected sharp increases in the auxin concentration in the root tip around day 8 (Marchant et al., 2002; Bhalerao et al., 2002). These increases are too late to influence the growth zone between days 2 and 6. In one of the studies, using long-day plants, such as the ones used here, the increased concentration of auxin in the root tip on day 8 was preceded by an increase in auxin concentration in the root near the root-shoot junction at day 6 (Bhalerao et al., 2002). A pulse of auxin in the shootward segments arriving at day 6 is also too late to explain the bursts of lateral root emergence in segments 1 to 3 (Figs 7, 8). The rate of lateral root emergence was affected around day 7 on segments 2 and 4 (Fig. 7B), an effect that could be temporally correlated with the arrival of the auxin pulse, but it is not clear how repeatable this is. It would be interesting to investigate whether the arrival of the auxin pulse contributes to ending the first period of growth zone development. A change in auxin level could be related to a change in *PLT* expression, either as cause or effect, because *PLT* expression promotes auxin synthesis and auxin promotes *PLT* expression over the long term (Santuari, et al., 2016; Mähönen et al., 2014). Long-term exposure to auxin also increases expression of *miR156* (Yu et al., 2015).

Does phase change occur in the root?

Phase change can be defined in many ways, but the general idea is that plants, like animals, go through distinct stages of development that can be characterized by a co-occurring group of attributes that are

regulated by a dedicated system. The idea that phase change may occur in the root is perhaps surprising as the type of organs produced by the root remains unchanged; however, age-dependent changes in root development have been widely observed. Many root crops, such as radish, undergo conspicuous secondary thickening as plants mature (Hoang et al., 2020). Even in *A. thaliana*, periclinal division of the cortical cells gives rise to a second cortical layer during the second week after germination (Dolan et al., 1993; Cui, 2016; Bertolotti et al., 2021). Another example of differential root development is found in maize, in which many of the genes that affect brace root formation also affect plant phase (Hostetler et al., 2021).

Here, a burst of *PLT2* expression that occurs around day 4 coordinates growth of the meristem and a delay in lateral root emergence (Figs 6, 9). These events are regulated by *miR156*. Because *miR156* regulates phase, being regulated by *miR156* is effectively synonymous with being regulated by the phase of the plant. Additional support for the involvement of the classical phase-change pathway in these coordinated developmental events in the root comes from prior work indicating that a *miR156*-resistant form of *SPL10* (*pSPL10:rSPL10*) prevents emergence of lateral roots for nearly 15 days (Yu et al., 2015). An *miR156*-resistant *SPL10* line also produces roots with an apparently longer meristem (Barrera-Rojas et al., 2020). Taken together, we argue that roots undergo phase change, and that the burst of *PLT2* that occurs around day 4 coordinates a brief phase of development between germination and juvenile vegetative growth, during which the meristem expands. We suggest that this period be called the seedling phase (Fig. 10).

Implications

The data presented here support the hypothesis that establishment of root meristems is a phase-regulated attribute of plant development, similar to leaf shape or trichome number in the shoot. The presence of phase-regulated aspects of development in the root further implies that roots undergo phase change. Being aware that roots have distinct phases is crucial to the design of research projects. Additionally, knowing that young seedlings have higher levels of *PLT3* expression and lower *PLT2* has implications for efforts to increase regeneration in older recalcitrant plants, and may provide ideas for regulating the rate at which the first lateral roots emerge, a factor that can impact seedling establishment and susceptibility to

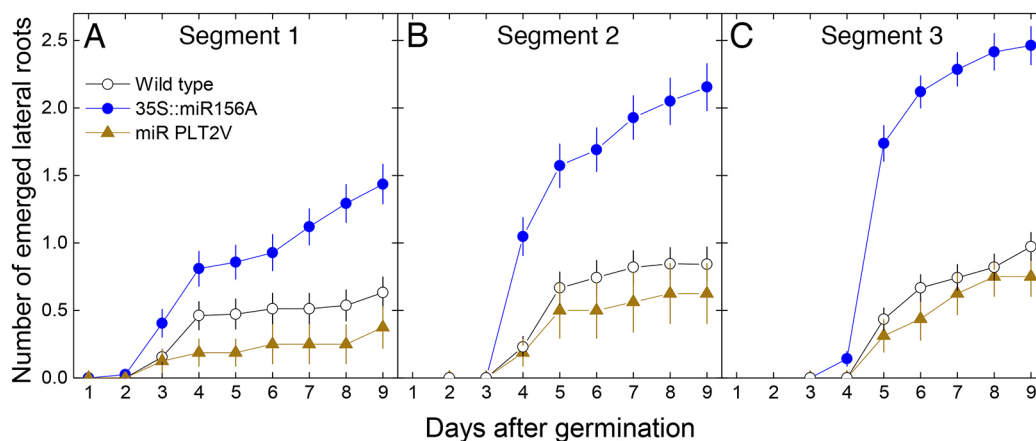


Fig. 8. *PLT2* slows the rate of lateral root emergence during early development. (A–C) The number of emerged lateral roots present on a single set of roots of wild type, *35S::miR156A* or *35S::miR156A PLT2-Venus* plants was recorded daily on segment 1 (A), segment 2 (B) and segment 3 (C). Segments are as defined in Fig. 7. Symbols represent the mean of 16–42 roots \pm s.e.m. The number of emerged lateral roots in *35S::miR156A* was found to be statistically different ($P < 0.05$ in a two-tailed Student's *t*-test) from wild type and from *35S::miR156A PLT2-Venus* from day 4 onwards in segments 1 and 2 (A,B), and from day 5 onward in segment 3 (C).

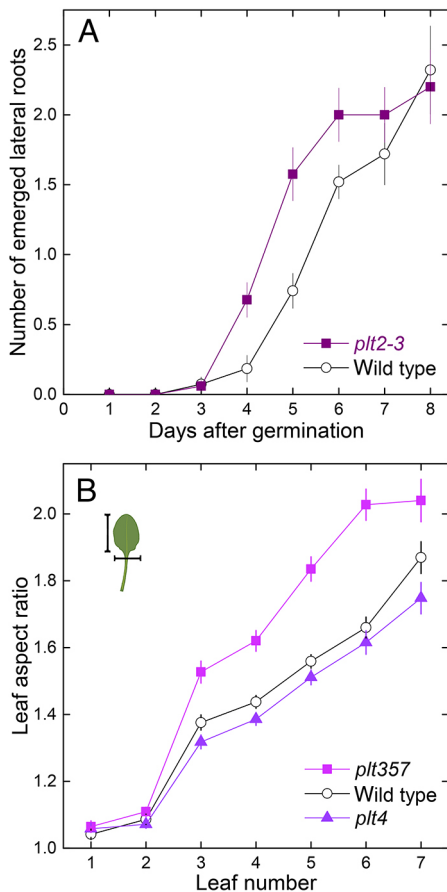


Fig. 9. PLETHORA genes affect the timing of lateral root emergence and leaf aspect ratio. (A) Lateral root emergence. The number of emerged lateral roots in *plt2-3* is statistically different ($P < 0.01$) from the number in wild-type roots for days 4 and 5, based on a two-tailed Student's *t*-test. Symbols represent the mean of 25–35 roots \pm s.e.m., except wild type day 8, which had 19 roots. (B) Leaf aspect ratio. Individual plants were dissected and the length and width of each successive leaf was measured. Symbols represent mean \pm s.e.m. of 26 *plt3plt5plt7* triple mutant (*plt357*), 29 wild type, or 30 *plt4* (*bbm1-1*) plants. That the ratio in the triple mutant equals that of the wild type is rejected at $P < 0.01$ for leaves 3 to 6 by a Student's *t*-test using the Bonferroni correction for multiple tests.

broadcast herbicides. The massive density of the *35S::miR156A* root system is of particular interest, especially as some of the increase is maintained even when the root system is grafted onto other shoot systems, as this may allow for the generation of plants that can more effectively store carbon in the soil.

MATERIALS AND METHODS

Plant lines and constructs

A. thaliana L. (Heynh) ecotype Columbia were grown on vertically oriented agar plates (with $1/2 \times$ MS, pH 5.8 with MES, 1% sucrose and 1.5% agar) at 23.8°C with 16 h light/8 h dark, unless otherwise noted. The *35S::miR156A* seed was a gift from Scott Poethig (University of Pennsylvania, PA, USA); *tem1em2* (Osnato et al., 2012) was a gift from Soraya Pelaz (CRAG Centre for Research in Agricultural Genomics, Barcelona); the *PLT3* promoter used for *PLT3::GUS* was described by Galinha et al. (2007), and its GUS fusion, as well as *PLT2-Venus* were gifts from Yujuan Du [Institute of Plant Sciences Paris-Saclay (IPS2), France]; and *plt3plt5plt7* triple mutants (Prasad et al., 2011) and *bbm1-1* (Galinha et al., 2007) were from Viola Willemsen (Wageningen University & Research, The Netherlands).

CRISPR/Cas9-mediated mutagenesis was used to generate the *PLT2* knock-out allele *plt2-3*. A construct was generated using Golden

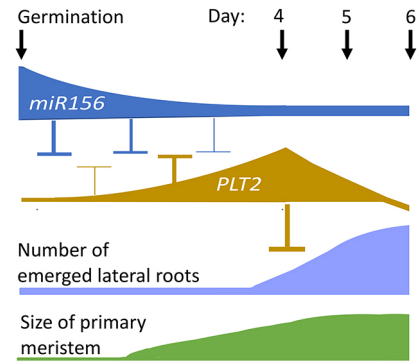


Fig. 10. Model of the regulatory network between *miR156* and *PLT2*. At the point of germination, seedlings express the juvenility factor *miR156* at a high level. High *miR156* expression inhibits *PLT2* expression, levels of which are low, but present, at germination. In turn, *PLT2* expression represses *miR156*; lower levels of *miR156* may result in less repression of *PLT2*, generating a self-reinforcing loop. Given the starting conditions, this regulatory network could explain the observed increase of *PLT2* expression between germination and day 4. *PLT2* expression delays lateral root emergence, resulting in a burst of lateral root emergence as *PLT2* levels decline. Because high levels of *PLT2* expression promote growth of the root meristem, this network also generates a period of meristem expansion. Although a decline in *PLT2* levels after day 4 was observed, the factors that lead to that decline have not yet been identified.

Gate cloning (Engler et al., 2014; Nekrasov et al., 2013), harboring two sgRNAs. Unless otherwise stated, plasmids originated from the MoClo Toolkit and Plant Parts kit (Addgene plasmid #1000000044 and plasmid #1000000047). *pAGM4723-FAST-RPS5a::aCas9-PLT2sgRNA2-PLT2sgRNA3* was generated by using spacer sequences TGTGAAGAGTGAATGTGAGG and CTTAGGAGTGAGCAAATCGG to design forward sgRNA primers and amplify corresponding *PLT2sgRNA2* and *PLT2sgRNA3* using the *pICH86966::AtU6p::sgRNA_PDS* construct (Addgene plasmid #46966) as a template. PCR products were combined with AtU6-26 promoter from level 0 plasmid *pICSL90002* (Addgene plasmid #68261) into level 1 vectors *pICH47751* and *pICH47761*, respectively. Subsequently, level 1 vectors harboring sgRNAs were combined with *pICH47732-FAST_R* (red seed selection) and *pICH47742-RPS5a::aCas9* and the end linker *pICH41780* into level 2 binary vector *pAGM4723*. Plasmid *pICH47732-FAST_R* was generated by Golden Gate cloning of the *pFAST-R* selection cassette from *pICSL7008* (monomeric tagRFP from *Entacmaea quadricolor* fused to the coding sequence of *AtOLE1*) into *pISCH47732*. Plasmid *pICH47742-RPS5a::aCas9* was generated by assembling *pICH41233-RPS5a*, *pICH41308-aCas9* and *pICH41421(nosT)* into *pICH47742*. The *RPS5a* promoter was amplified using pRPS5AF-BpiGGAG (TGTGAAGACAAGGAGCTCAACTTTT-GATTTCGCTATTTG) and pRPS5AR-BpiTACT (TGTGAAGACAAGGAGCTGTGGTGAGAGAAACAGA) followed by Golden Gate cloning into *pICH41233*. A plasmid harboring the *A. thaliana* codon optimized *aCas9* was kindly provided by the Puchta lab (Fauser et al., 2014) and amplified using a Cas9F-BpiAATG (TGTGAAGACAAAATGGATAA-GAAGTACTCTATCGGACTC) and a Cas9R-BpiGCTT (TGTGAAGACAAAAGCTCAAACCTTCTCTCTTCTTAGG) followed by Golden Gate cloning into *pICH41308*.

Columbia plants were transformed by floral dip (Clough and Bent, 1998), and T1 transgenic seeds selected under a fluorescence binocular. Inflorescences of T1 plants were genotyped for induced mutation by PCR using primers *plt2-3F* (CCAACTTGCGTTTCTCAAA) and *plt2-3R* (AGAGGCACAAGTGACGACTG) followed by sequencing (Table S1). Seeds of mutant plants were selected for absence of the CRISPR/Cas9 construct followed by genotyping for homozygosity of the mutation. The *plt2-3* allele is characterized by a single A nucleotide insertion at 80 bp into the second exon thereby creating a frameshift and an early stop codon 14 aa downstream.

Growth conditions

Seeds were sterilized in 70% ethanol, followed by 12–15 min in 2.6% sodium hypochlorite, and four washes in sterile deionized water, prior to being stored at 4°C for about 72 h. The morning following seeding, plates were placed under a dissecting microscope and those with emerged radicles were marked as germinated. Germination checks continued at 12 h intervals until a sufficiently large cohort of seeds germinating in one 12 h window was obtained. This time was defined as time zero, and only that cohort was followed for the rest of the experiment, ensuring that plants harvested on a given day would be at the same developmental age. Roots were excluded from the experiments based on pre-established guidelines. Roots were excluded if they: (1) grew into the agar rather than on top of it, (2) grew off the agar into the air, (3) fell off the agar, (4) ran into the edge of the plate, (5) died in part or whole, or (6) were on plates that were visibly infected.

Ticking experiments

The position of the root tip was marked at daily intervals. A plate holder in the growth chamber was set to eye level, and scratches were made on the back of the plate with a razor blade to indicate the position of the root tip. At the end of the experiment, plates were photographed using a digital camera. Root lengths and angles were measured using ImageJ (Schneider et al., 2012).

GUS staining

For experiments involving GUS stain, plates were placed in a horizontal position and substrate solution (Willemsen et al., 1998) was gently pipetted over each plant. Plates were wrapped in foil and left at 37°C for 45 min to 16 h, with the time varying by experiment, prior to being placed on a glass microscope slide in water, or, for *miR156C::GUS* in Fig. 4, in ice-cold chloral hydrate. Roots were photographed on a Zeiss Axioscope or an Olympus SZX7 dissecting microscope with cellSens Standard software. The intensity of *PLT3::GUS* staining was determined using ImageJ to calculate mean intensity of the inverted red channel for a region of interest that fit within the meristem (Fig. S3).

Cortical cell length and cell production rates

Cell length was measured in propidium iodide-stained roots under a Zeiss LSM Pascal 5 confocal microscope, using the built-in image analysis software. This population was germination checked at 24 h intervals. Cortical cell measurements began at the first cell shootward of an emerged root hair, and images were taken along the root in the shootward direction until approximately 20 cortical cells were obtained; in younger roots, the number of cortical cells that could be measured in a given root was often fewer than 20. Measured cells were averaged for each root. Reported values reflect the averages and s.e.m. of values for eight (or in one case nine) roots per genotype per day. Cell production rates were calculated as: average root elongation rate ($\mu\text{m}/\text{day}$) divided by average mature cell length ($\mu\text{m}/\text{cell}$) = cells/day (Baskin, 2013). Errors were propagated by calculating the fractional error for each initial value and then taking the square root of the sum of the squares. The resulting value was then multiplied by the cell production rate to obtain the error (<http://www.upscale.utoronto.ca/PVB/Harrison/ErrorAnalysis/>).

Kinematic analysis of root growth

For kinematic analysis, the root tip was imaged through a 10 \times objective. For each root, eight images were acquired, separated by 10 s. The time that any plate spent in the horizontal position was restricted to 10 min or less. After imaging, the plate was returned to the growth chamber. Later, velocity profiles were generated for each pair of images separated by 40 s using Stripflow software (Baskin and Zelinsky, 2019). For each root, the four velocity profiles thus obtained were averaged. Then, the average profile was fitted to a modified sigmoidal function (Peters and Baskin, 2006). Fitted values for four parameters are reported here. First is maximal velocity, which is equivalent to root growth rate. The second is relative elongation rate (often called ‘cell elongation rate’), obtained from the slope of the profile within the elongation zone where velocity increases steeply and almost

linearly. The third is meristem length, taken as the position where the velocity profile transitions between regions of gradual and steep increase; this length includes a short region adjacent to the meristem where cells no longer divide. Finally, the fourth is growth zone length, taken as the position where the velocity profile transitions between regions of steep increase and constancy; constant velocity means zero relative elongation and hence represents the mature zone (Baskin and Zelinsky, 2019).

Grafting and rhizotrons

Plants were germinated on agar plates without sucrose, and seedlings were grafted when the first leaves were emerging as described by Melnyk (2017). Approximately 1 week after grafting, grafts were tested by gently pulling on the shoot: those that held together and showed no signs of adventitious root formation were transferred to agar plates or rhizotrons and grown until maturity (~6 weeks). Rhizotrons were prepared by placing a thin foam spacer between two sheets of safety glass and wrapping three edges of the glass in Micropore tape (3M). The space between the glass was filled with dry soil (Just Natural Organic All Purpose Garden Soil, Oldcastle Lawn & Garden, Inc., Atlanta, GA, USA) that had been passed through a sieve to remove large particles and baked overnight at 60°C. Packing of soil was promoted by repeatedly pounding the sealed bottom of the rhizotrons on the floor; additional soil was then added to the top until the structure was full. Filled rhizotrons were submerged overnight in water containing approximately one capful per 66 l water of Miracle-Gro All Purpose Plant Food (Miracle-Gro Lawn Products Inc., Marysville, OH, USA). Rhizotrons were then wrapped in foil, leaving an opening along the narrow strip of soil at the top, planted, and placed in the growth chamber at about a 45° angle. To assay root density, foil was removed and rhizotrons were imaged from the previously lower side against which the roots had grown. The perimeter of each root system was drawn by eye, and the average mean gray value of the pixels inside the resulting shape was determined using ImageJ (Schneider et al., 2012). To control for between-rhizotron differences, the density of each root system is reported relative to wild type. For Fig. 5B bottom (*35S::miR156A* versus *35S::miR156 plt2-3*), the sample size was increased from five to 15 after the initial group size proved to be underpowered.

Confocal microscopy

Confocal laser-scanning microscopy images of *PLT2-Venus* were obtained on a Zeiss LSM 880 Airyscan confocal laser-scanning microscope using an LD LCI Plan Apochromat 40 \times /1.2 immersion-corrected DIC objective. Roots were placed on a coverslip in a drop of water or propidium iodide (1 $\mu\text{g}/\text{ml}$, to stain the cell walls and visualize the root meristem). The root tip was imaged using the tile scan function in Zen Black. Single-channel grayscale images were exported from ZEN Black and opened in ImageJ. Mean gray intensity was measured over a rectangular region of interest that covered the stem cell niche (Fig. S3).

Real-time PCR

Plants were grown on agar plates for the indicated number of days. For *PLT2* expression, germination checking was carried out between 08:00 and 09:00 and between 17:00 and 18:00 until the experimental cohort was identified. At harvest, roots were cut at approximately 0.4 cm above the root tip (day 2) or 0.5 cm above the root tip (days 4 and 6) and frozen in liquid nitrogen. Approximately 100–250 root tips were collected per time point. Samples, to which a glass bead was added, were ground with a SPEX SamplePrep 2010 (Geno/Grinder) at 1500 rpm for two 1 min bursts, with a period of re-freezing between the bursts. RNA was extracted using the Aurum Total RNA Mini Kit (Bio-Rad). The cDNA was synthesized using an iScript cDNA synthesis kit (Bio-Rad) based on 0.3–1 μg RNA, with equivalent amounts for all samples within a trial. The qPCR was run by using SsoAdvanced Universal SYBR Green Supermix (Bio-Rad) and primers (Table S1) from IDT in a Bio-Rad iCycler iQ (95°C for 3 min, followed by 40 cycles of 95°C for 10 s and 60°C for 45 s, and then single periods of 95°C for 1 min and 55°C for 1 min; following amplification, a melt curve was obtained). The threshold cycle (C_t) was determined automatically by the instrument, *TUBULIN 2* (*TUB2*) was used for calibration, and fold

changes were calculated as follows:

$$\text{Fold change} = 2^{\frac{(C_{\text{test, reference}} - C_{\text{test, target}})}{(C_{\text{calibrate, reference}} - C_{\text{calibrate, target}})}}$$

Leaf shape

Plants were grown in soil until they had nine leaves, when they were uprooted and inverted. Leaves were removed from the base of the shoot (first formed) to the innermost (upper, most recently formed) with the aid of a dissecting microscope, and then affixed to a sheet of clear Plexiglas using double-sided tape. Leaves were scanned on a Konica Minolta Bizhub 654e machine, and images quantified using ImageJ (Schneider et al., 2012). Maximum length and width were recorded.

Acknowledgements

We thank the National Science Foundation for funding the purchase of the confocal (MRI 1828041); Greg Lee for helpful conversations; Zofia Stanley for statistical advice; Laura Green for help drawing figures; Andrea Paterlini for teaching us how to graft; Davy Opendacker and Tom Beeckman along with Kavya Yalamanchili and Ikram Bilou for showing us how to make mini-rhizotrons; Scott Poethig for 35S::miR156A; Soraya Pelaz for *tem1tem2*; Carlos Barrera-Rojas and Fabio Tebaldi Silveira Nogueira for *pmiR156A::GUS* and *pmiR156C::GUS* lines and technical advice; Ben Scheres' lab for *PLT* mutant and reporter lines; and Connie Estevez and undergraduate students in Oberlin College BIOL 204 and BIOL 221 for preliminary experiments.

Competing interests

The authors declare no competing or financial interests.

Author contributions

Conceptualization: M.J.L., O.L.; Validation: Y. Fang; Formal analysis: M.J.L., H.C.T., Y. Fang, P.B.; Investigation: M.J.L., H.C.T., T.I.B., Y. Fang, A.E., Y. Fu, R.R., T.J.D.; Resources: R.H., T.I.B., O.L.; Writing - original draft: M.J.L.; Writing - review & editing: T.I.B., H.C.T., R.H., Y.F.; Visualization: M.J.L., H.C.T., T.I.B.; Supervision: M.J.L., T.I.B.; Project administration: M.J.L.; Funding acquisition: M.J.L.

Funding

This work was funded by the National Science Foundation (IOS 1656621 to M.J.L.) Open Access funding provided by the National Science Foundation. Deposited in PMC for immediate release.

References

- Aguilar-Jaramillo, A. E., Marín-González, E., Matías-Hernández, L., Osnato, M., Pelaz, S. and Suárez-López, P. (2019). TEMPRANILLO is a direct repressor of the microRNA miR172. *Plant J.* **100**, 522-535. doi:10.1111/tpj.14455
- Aida, M., Beis, D., Heidstra, R., Willemsen, V., Bilou, I., Galinha, C., Nussaume, L., Noh, Y.-S., Amasino, R. and Scheres, B. (2004). The PLETHORA genes mediate patterning of the Arabidopsis root stem cell niche. *Cell* **119**, 109-120. doi:10.1016/j.cell.2004.09.018
- Barrera-Rojas, C. H., Rocha, G. H. B., Polverari, L., Brito, D. A. P., Batista, D. S., Notini, M. M., Ferreira da Cruz, A. C., Morea, E. G. O., Sabatini, S., Otoni, W. C. et al. (2020). miR156-targeted SPL10 controls Arabidopsis root meristem activity and root-derived de novo shoot regeneration via cytokinin responses. *J. Exp. Bot.* **71**, 934-950. doi:10.1093/jxb/erz475
- Baskin, T. I. (2013). Patterns of root growth acclimation: constant processes, changing boundaries. *WIREs Dev. Biol.* **2**, 65-73. doi:10.1002/wdev.94
- Baskin, T. I. and Zelinsky, E. (2019). Kinematic characterization of root growth by means of Stripflow. In *Plant Cell Morphogenesis: Methods and Protocols*, 2nd edn. (ed. F. Cvrčková and V. Žárský), pp.291-305. New York: Humana.
- Beemster, G. T. S. and Baskin, T. I. (1998). Analysis of cell division and elongation underlying the developmental acceleration of root growth in *Arabidopsis thaliana*. *Plant Physiol.* **116**, 1515-1526. doi:10.1104/pp.116.4.1515
- Bertolotti, G., Unterholzner, S. J., Scintu, D., Salvi, E., Svolacchia, N., Di Mambro, R., Ruta, V., Linhares Scaglia, F., Vittorioso, P., Sabatini, S. et al. (2021). A PHABULOSA-controlled genetic pathway regulates ground tissue patterning in the Arabidopsis root. *Curr. Biol.* **31**, 420-426.e6. doi:10.1016/j.cub.2020.10.038
- Bhalerao, R. P., Eklöf, J., Ljung, K., Marchant, A., Bennett, M. and Sandberg, G. (2002). Shoot-derived auxin is essential for early lateral root emergence in Arabidopsis seedlings. *Plant J.* **29**, 325-332. doi:10.1046/j.0960-7412.2001.01217.x
- Cheng, Y.-J., Shang, G.-D., Xu, Z.-G., Yu, S., Wu, L.-Y., Zhai, D., Tian, S.-L., Gao, J., Wang, L. and Wang, J.-W. (2021). Cell division in the shoot apical meristem is a trigger for miR156 decline and vegetative phase transition in *Arabidopsis*. *Proc. Natl. Acad. Sci. USA* **118**, e2115667118. doi:10.1073/pnas.2115667118
- Clough, S. J. and Bent, A. F. (1998). Floral dip: a simplified method for Agrobacterium-mediated transformation of *Arabidopsis thaliana*. *Plant J.* **16**, 735-743. doi:10.1046/j.1365-313x.1998.00343.x
- Cui, H. (2016). Middle cortex formation in the root: an emerging picture of integrated regulatory mechanisms. *Mol. Plant* **9**, 771-773. doi:10.1016/j.molp.2016.05.002
- Dolan, L., Janmaat, K., Willemsen, V., Linstead, P., Poethig, S., Roberts, K. and Scheres, B. (1993). Cellular organisation of the *Arabidopsis thaliana* root. *Development* **119**, 71-84. doi:10.1242/dev.119.1.71
- Du, Y. (2017). The regulation of Arabidopsis thaliana lateral root development by redundant PLETHORA transcription factors. *PhD thesis*, Wageningen University Research, The Netherlands.
- Du, Y. and Scheres, B. (2017). PLETHORA transcription factors orchestrate de novo organ patterning during Arabidopsis lateral root outgrowth. *Proc. Natl. Acad. Sci. USA* **114**, 11709-11714. doi:10.1073/pnas.1714410114
- Du, Y. and Scheres, B. (2018). Lateral root formation and the multiple roles of auxin. *J. Exp. Bot.* **69**, 155-167. doi:10.1093/jxb/erx223
- Engler, C., Youles, M., Gruetzner, R., Ehnert, T.-M., Werner, S., Jones, J. D. G., Patron, N. J. and Marillonnet, S. (2014). A Golden Gate modular cloning toolbox for plants. *ACS Synth. Biol.* **3**, 839-843. doi:10.1021/sb4001504
- Fausser, F., Schiml, S. and Puchta, H. (2014). Both CRISPR/Cas-based nucleases and nickases can be used efficiently for genome engineering in *Arabidopsis thaliana*. *Plant J.* **79**, 348-359. doi:10.1111/tpj.12554
- Galinha, C., Hofhuis, H., Luijten, M., Willemsen, V., Bilou, I., Heidstra, R. and Scheres, B. (2007). PLETHORA proteins as dose-dependent master regulators of Arabidopsis root development. *Nature* **449**, 1053-1057. doi:10.1038/nature06206
- Gao, R., Wang, Y., Gruber, M. Y. and Hannoufa, A. (2018). miR156/SPL10 modulates lateral root development, branching and leaf morphology in Arabidopsis by silencing AGAMOUS-LIKE 79. *Front. Plant. Sci.* **8**, 2226. doi:10.3389/fpls.2017.02226
- Hoang, N. V., Choe, G., Zheng, Y., Aliaga, A. C., Fandiño, A. C. A., Sung, I., Hur, J., Kamran, M., Park, C., Kim, H. et al. (2020). Identification of conserved gene-regulatory networks that integrate environmental sensing and growth in the root cambium. *Curr. Biol.* **30**, 2887-2900. doi:10.1016/j.cub.2020.05.046
- Hofhuis, H., Laskowski, M., Du, Y., Prasad, K., Grigg, S., Pinon, V. and Scheres, B. (2013). Phyllotaxis and rhizotaxis in Arabidopsis are modified by three PLETHORA transcription factors. *Curr. Biol.* **23**, 956-962. doi:10.1016/j.cub.2013.04.048
- Horstman, A., Fukuoka, H., Muino, J. M., Nitsch, L., Guo, C., Passarinho, P., Sanchez-Perez, G., Immink, R., Angenent, G. and Boutilier, K. (2015). ALL and HDG proteins act antagonistically to control cell proliferation. *Development* **142**, 454-464. doi:10.1242/dev.117168
- Horstman, A., Li, M., Heidmann, I., Weemen, M., Chen, B., Muino, J. M., Angenent, G. C. and Boutilier, K. (2017). The BABY BOOM transcription factor activates the LEC1-ABI3-FUS3-LEC2 network to induce somatic embryogenesis. *Plant Physiol.* **175**, 848-857. doi:10.1104/pp.17.00232
- Hostetler, A. N., Khangura, R. S., Dilkes, B. P. and Sparks, E. E. (2021). Bracing for sustainable agriculture: the development and function of brace roots in members of Poaceae. *Curr. Opin. Plant Biol.* **59**, 101985. doi:10.1016/j.pbi.2020.101985
- Kareem, A., Durgaprasad, K., Sugimoto, K., Du, Y., Pulianmackal, A. J., Trivedi, Z. B., Abhayadev, P. V., Pinon, V., Meyerowitz, E. M., Scheres, B. et al. (2015). PLETHORA genes control regeneration by a two-step mechanism. *Curr. Biol.* **25**, 1017-1030. doi:10.1016/j.cub.2015.02.022
- Mähönen, A. P., ten Tusscher, K., Siligato, R., Smetana, O., Díaz-Triviño, S., Salojärvi, J., Wachsmann, G., Prasad, K., Heidstra, R. and Scheres, B. (2014). PLETHORA gradient formation mechanism separates auxin responses. *Nature* **515**, 125-129. doi:10.1038/nature13663
- Marchant, A., Bhalerao, R., Casimiro, I., Eklöf, J., Casero, P. J., Bennett, M. and Sandberg, G. (2002). AUX1 promotes lateral root formation by facilitating indole-3-acetic acid distribution between sink and source tissues in the Arabidopsis seedling. *Plant Cell* **14**, 589-597. doi:10.1105/tpc.010354
- Melnyk, C. W. (2017). Grafting with *Arabidopsis thaliana*. *Methods Mol. Biol.* **1497**, 9-18. doi:10.1007/978-1-4939-6469-7_2
- Moubayidin, L., Perilli, S., Dello Iorio, R., Di Mambro, R., Costantino, P. and Sabatini, S. (2010). The rate of cell differentiation controls the Arabidopsis root meristem growth phase. *Curr. Biol.* **20**, 1138-1143. doi:10.1016/j.cub.2010.05.035
- Moubayidin, L., Salvi, E., Giustini, L., Terpstra, I., Heidstra, R., Costantino, P. and Sabatini, S. (2016). A SCARECROW-based regulatory circuit controls Arabidopsis thaliana meristem size from the root endodermis. *Planta* **243**, 1159-1168. doi:10.1007/s00425-016-2471-0
- Nekrasov, V., Staskawicz, B., Weigel, D., Jones, J. D. G. and Kamoun, S. (2013). Targeted mutagenesis in the model plant *Nicotiana benthamiana* using Cas9 RNA-guided endonuclease. *Nat. Biotech.* **31**, 691-693. doi:10.1038/nbt.2655
- Osnato, M., Castillejo, C., Matías-Hernández, L. and Pelaz, S. (2012). TEMPRANILLO genes link photoperiod and gibberellin pathways to control flowering in Arabidopsis. *Nat. Commun.* **3**, 808. doi:10.1038/ncomms1810

- Peters, W. S. and Baskin, T. I. (2006). Tailor-made composite functions as tools in model choice: the case of sigmoidal vs bi-linear growth profiles. *Plant Methods* **2**, 11. doi:10.1186/1746-4811-2-11
- Pi, L., Aichinger, E., van der Graaff, E., Llavata Peris, C. I., Weijers, D., Hennig, L., Groot, E. and Laux, T. (2015). Organizer-derived WOX5 signal maintains root columella stem cells through chromatin-mediated repression of CDF4 expression. *Dev. Cell* **33**, 576-588. doi:10.1016/j.devcel.2015.04.024
- Poethig, S. R. (2013). Vegetative phase change and shoot maturation in plants. *Curr. Top. Dev. Biol.* **105**, 125-152. doi:10.1016/B978-0-12-396968-2.00005-1
- Prasad, K., Grigg, S. P., Barkoulas, M., Yadav, R. K., Sanchez-Perez, G. F., Pinon, V., Blilou, I., Hofhuis, H., Dhonukshe, P., Galinha, C. et al. (2011). Arabidopsis PLETHORA transcription factors control phyllotaxis. *Curr. Biol.* **21**, 1123-1128. doi:10.1016/j.cub.2011.05.009
- Radhakrishnan, D., Shanmukhan, A. P., Kareem, A., Aiyaz, M., Varapparambathu, V., Toms, A., Kerstens, M., Valsakumar, D., Landge, A. N., Shaji, A. et al. (2020). A coherent feed forward loop drives vascular regeneration in damaged aerial organs growing in normal developmental-context. *Development* **147**, 1477-9129. doi:10.1242/dev.185710
- Salvi, E., Rutten, J. P., Di Mambro, R., Polverari, L., Licursi, V., Negri, R., Dello Iorio, R., Sabatini, S. and Ten Tusscher, K. (2020). A self-organized PLT/Auxin/ARR-B network controls the dynamics of root zonation development in Arabidopsis thaliana. *Dev. Cell* **53**, 431-443.e23. doi:10.1016/j.devcel.2020.04.004
- Santuari, L., Sanchez-Perez, G. F., Luijten, M., Rutjens, B., Terpstra, I., Berke, L., Gorte, M., Prasad, K., Bao, D., Timmermans-Hereijgers, J. L. et al. (2016). The PLETHORA gene regulatory network guides growth and cell differentiation in Arabidopsis roots. *Plant Cell* **28**, 2937-2951. doi:10.1105/tpc.16.00656
- Sarkar, A. K., Luijten, M., Miyashima, S., Lenhard, M., Hashimoto, T., Nakajima, K., Scheres, B., Heidstra, R. and Laux, T. (2007). Conserved factors regulate signaling in Arabidopsis thaliana shoot and root stem cell organizers. *Nature* **446**, 811-814. doi:10.1038/nature05703
- Schneider, C. A., Rasband, W. S. and Eliceiri, K. W. (2012). NIH Image to ImageJ: 25 years of image analysis. *Nat. Methods* **9**, 671-675. doi:10.1038/nmeth.2089
- Shimotohno, A., Heidstra, R., Blilou, I. and Scheres, B. (2018). Root stem cell niche organizer specification by molecular convergence of PLETHORA and SCARECROW transcription factor modules. *Genes Dev.* **32**, 1085-1100. doi:10.1101/gad.314096.118
- Wang, J. W., Park, M. Y., Wang, L.-J., Koo, Y., Chen, X.-Y., Weigel, D. and Poethig, S. R. (2011). MIRNA control of vegetative phase change in trees. *PLoS Genet.* **7**, e1002012. doi:10.1371/journal.pgen.1002012
- Willemsen, V., Wolkenfelt, H., de Vrieze, G., Weisbeek, P. and Scheres, B. (1998). The HOBBIT gene is required for formation of the root meristem in the Arabidopsis embryo. *Development* **125**, 521-531. doi:10.1242/dev.125.3.521
- Wu, G. and Poethig, R. S. (2006). Temporal regulation of shoot development in Arabidopsis thaliana by miR156 and its target SPL3. *Development* **133**, 3539-3547. doi:10.1242/dev.02521
- Wu, G., Park, M. Y., Conway, S. R., Wang, J. W., Weigel, D. and Poethig, R. S. (2009). The sequential action of miR156 and miR172 regulates developmental timing in Arabidopsis. *Cell* **138**, 750-759. doi:10.1016/j.cell.2009.06.031
- Xu, M., Hu, T., Zhao, J., Park, M.-Y., Earley, K. W., Wu, G. and Scott, P. R. (2016a). Developmental functions of miR156-regulated SQUAMOSA PROMOTER BINDING PROTEIN-LIKE (SPL) genes in Arabidopsis thaliana. *PLoS Genet.* **12**, e1006263. doi:10.1371/journal.pgen.1006263
- Xu, M., Hu, T., Smith, M. R. and Poethig, R. S. (2016b). Epigenetic regulation of vegetative phase change in Arabidopsis. *Plant Cell* **28**, 28-41. doi:10.1105/tpc.15.00854
- Xu, M., Leichty, A. R., Hu, T. and Poethig, R. S. (2018a). H2A.Z promotes the transcription of MIR156A and MIR156C in Arabidopsis by facilitating the deposition of H3K4me3. *Development* **145**, dev152868. doi:10.1242/dev.152868
- Xu, Y., Zhang, L. and Wu, G. (2018b). Epigenetic regulation of juvenile-to-adult transition in plants. *Front. Plant Sci.* **9**, 1048. doi:10.3389/fpls.2018.01048
- Yu, S., Galvão, V. C., Zhang, Y.-C., Horrer, D., Zhang, T.-Q., Hao, Y.-H., Feng, Y.-Q., Wang, S., Schmid, S. M. and Wang, J.-W. (2012). Gibberellin regulates the Arabidopsis floral transition through miR156-targeted SQUAMOSA PROMOTER BINDING-LIKE transcription factors. *Plant Cell* **24**, 3320-3332. doi:10.1105/tpc.112.101014
- Yu, N., Niu, Q. W., Ng, K. H. and Chua, N. H. (2015). The role of miR156/SPLs modules in Arabidopsis lateral root development. *Plant J.* **83**, 673-685. doi:10.1111/tpj.12919

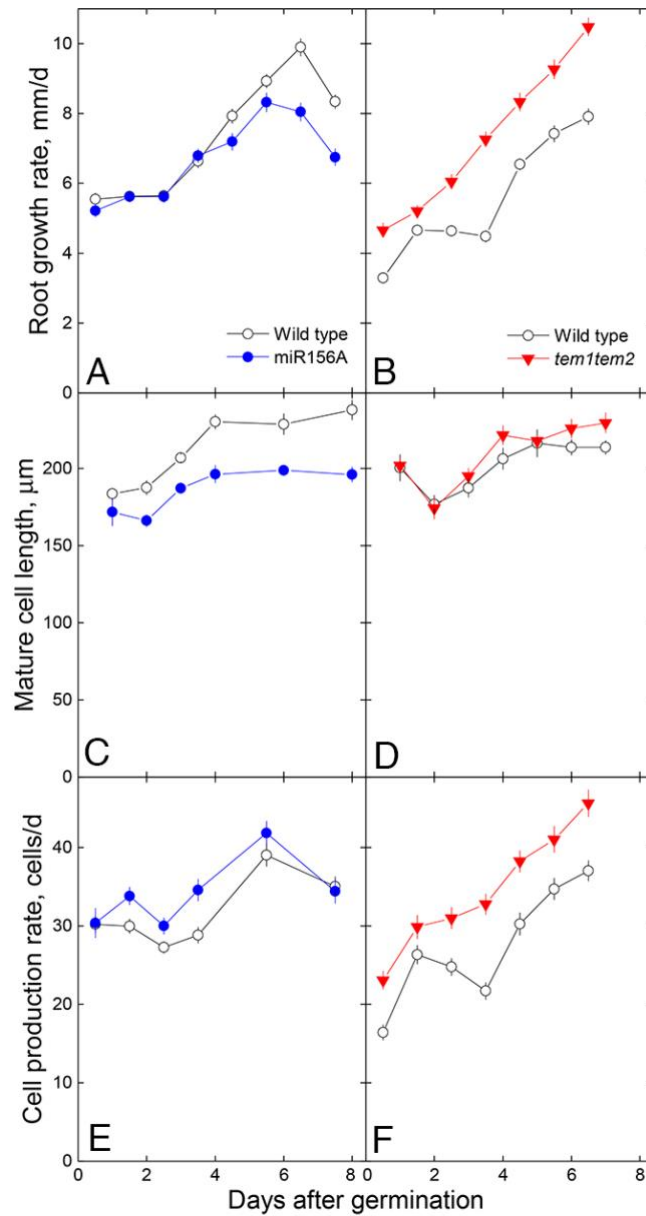


Fig. S1. Rates of growth and mature cell length vary as roots mature and are affected by known phase change regulators (A) Growth rate of wild type (n = 38) and *35S::miR156A* (n = 37) roots, and (B) wild type (n = 31) and *tem1tem2* double mutant (n = 28) roots. (C, D) Length of mature cortical cells in the indicated genotypes. Symbols represent means of 8 or 9 roots \pm s.e.m.. (E, F) Number of cells produced per day, calculated from data in A – D.

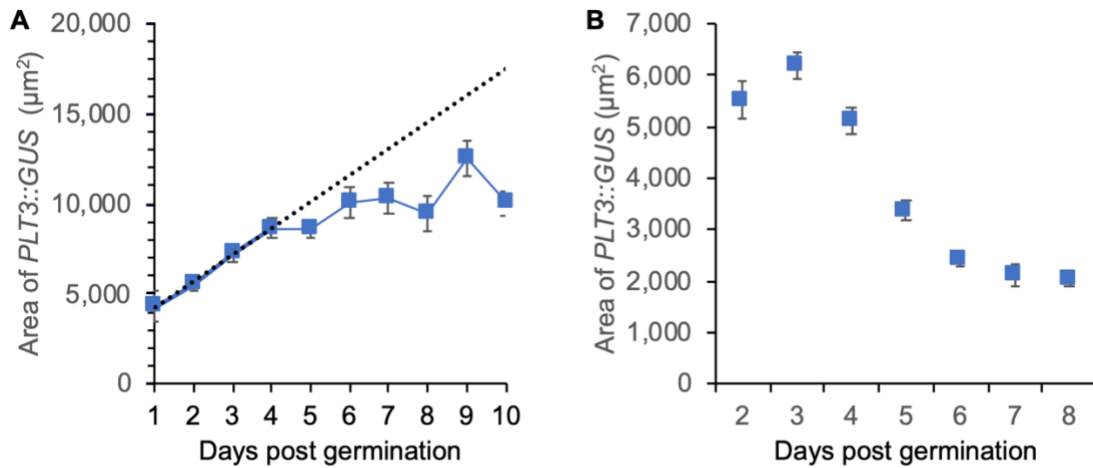


Fig. S2. The area of *PLT3::GUS* expression at the site of a lateral root primordium increases more slowly, or declines, after day 4. Each data point reflects the average area in which *PLT3::GUS* stain is visible around the presumptive site of a lateral root primordium. Data are (A) from the region of root that grew in the most recent 24 h. (On day 1, this is segment 1 as defined in Figure 5; on day 2 it is segment 2, and so on). (B) Data from the region that grew in the 24 h before that (No such region exists on day 1; on day 2, it is segment 1; on day 3 it is segment 2 and so on). Each point reflects the average of all the GUS-stained spots in the segments from 8 -10 roots \pm s.e.m.. The decline in area was driven by decreased width of individual spots, where width runs parallel to the long axis of the root. Data from plants in this trial are also included in Table 1.

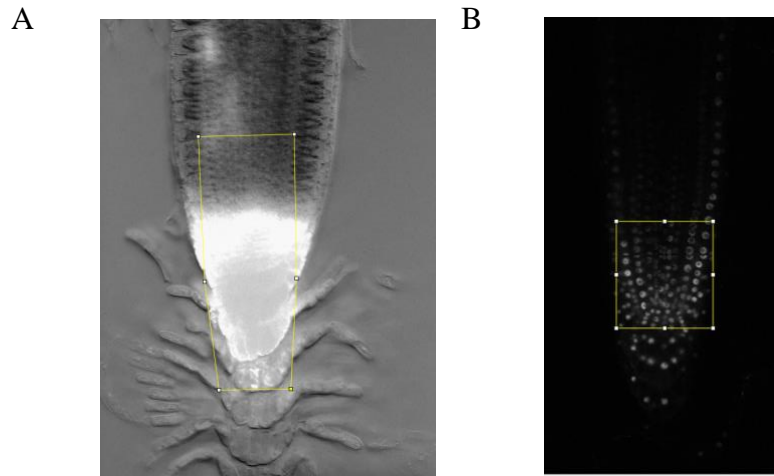


Fig. S3. Quantification of GUS staining and Venus fluorescence in Figure 3. Representative image showing the region of interest (ROI) used for quantification of (A) *PLT3::GUS* staining and (B) *PLT2*- VenusYFP fluorescence. (A) To quantify the blue signal in GUS stained roots, color images were opened in Image J, split into separate channels, and the red channel was inverted. The ROI was positioned as shown over the root tip and stem cell niche, and its mean gray level recorded. (B) For YFP fluorescence, single channel gray scale images were exported from Zen Black software and opened in Image J. The ROI was positioned such that the second narrow row of cells below the QC was included at the rootward end of the region, and the mean gray level of the region was recorded.

Table S1. Primer sequences.

| Primer name | Sequence |
|------------------------------------------------------|-----------------------------|
| Primer sequences for qPCR | |
| PLT2-F | CTTTGCCGCCTCACATTCAC |
| PLT2-R | TTTGGAACCTCTCCACCTTCG |
| PLT3-F | TCAGGAGGAAGAGTAGC |
| PLT3-R | TCTTTGTTCCCAGCAACTCG |
| TUB2-F | AGCAATACCAAGATGCAACTGCG |
| TUB2-R | TAACTAAATTATTCTCAGTACTCTTCC |
| Primer sequences for <i>plt2-3</i> genotyping | |
| <i>plt2-3 F</i> | CCAAACTTGCGTTTCTCAA |
| <i>plt2-3 R</i> | AGAGGCACAAGTGACGACTG |

PLT3 primers are from Du (2017).